METALLOGRAPHIC PROPERTIES OF YAMATO IRON METEORITE, YAMATO-75031, AND STONY-IRON METEORITE, YAMATO-74044

R. M. FISHER, C. E. SPANGLER, Jr.
U.S. Steel Research Laboratory, Monroeville, Pa. 15146, U.S.A.

and

T. NAGATA
National Institute of Polar Research, Kaga 1-chome, Itabashi-ku, Tokyo 173

Abstract: Chemical and metallographic examination of Yamato iron meteorite, Yamato-75031, has revealed that the major elements in the iron base are 15.3%Ni, 1%P, and 0.76%Co. Very large Fe-Ni phosphides (schreibersite) are enveloped with swathing kamacite and very fine phosphides are also encased in Widmanstätten kamacite plates within a plessite matrix. The composition and microstructure are quite similar to Piñon which is classified as an anomalous high nickel ataxite. Some annealing of the plessite occurred during entry into the earth's atmosphere.

Chemical and metallographic examination of Yamato stony-iron meteorite, Yamato-74044, has revealed that the major elements in the metal phase are 11%Ni, 0.1%P, 0.75%Co with adjacent pools of manganese-rich olivine veined with iron sulphide. The olivine component and the nickel content classify this stony iron as a pallasite. The nickel contents of the taenite and plessite indicate chemical equilibrium during cooling to 400°C. These samples, along with Yamato-75105, weighing from 20–60 grams, are smaller than any other iron or stony-iron meteorites.

1. Introduction

The details of the discovery of nearly 1,000 meteorite pieces in a limited area near the Yamato Mountains, now called the Meteorite Ice Field, have been described in detail (NAGATA, 1975; NAGATA *et al.*, 1976; YANAI 1975). Since the original discovery of nine pieces in 1969, Japanese Antarctic Research Expeditions have made special efforts to locate additional meteorite samples in this general area. During 1977 a joint U.S.-Japan field team searched a comparable blue ice area in the American sector and located eleven meteorites including one very large chondrite (CASSIDY *et al.*, 1977). The primary metallographic and magnetic properties of one of the Yamato iron meteorites, Yamato-75105, have been reported previously (NAGATA *et al.*, 1976). In this paper, we report on metallographic analysis of another Yamato iron and a stony-iron meteorite for comparison with the previously analyzed samples. More detailed studies of these samples including microprobe measurements are in progress and will be published separately.

As discussed previously (NAGATA *et al.*, 1976) the relative rate of sinking of meteorites in the ice after they fell is a function of their density and size. The larger, heavier meteorites sink more rapidly than either small or low-density meteorites so that they may sink too far to be exposed in the ablation zone region, and for this reason are lost for recovery.

2. General Description of Yamato-75031 Meteorite

The Yamato-75031 iron meteorite is approximately gumdrop-shaped with a mean diameter of about 4 cm, and an overall length of about 27 mm. The weight as found was 60.2 grams, with an apparent density of 7.470. The original piece was partitioned into two sections for magnetic and metallographic analysis. A photograph of the full cross-section is shown in Fig. 1. Very little porosity is noted in keeping with the high density of this metallic sample. The fusion crust is fairly fine-grained and is dark blue gray with some flecks of brown visible. This appearance is very similar to that of Yamato-75105. The hardness was found to vary from about 195 to 215 dph, which is in the low range for iron-nickel meteorites. Qualitative X-ray fluorescence analysis of the cross-section gives the following chemical composition:

Chemical composition.

	Si	Ni	Cu	Co	P	S	Al	Fe+O
Metal base	0.06	15.3	0.035	0.76	1.0	0.025	0.06	Remainder
	Mo, Nb, Cr, V, Ti, Mn<0.01%						(wt. %)	

The nickel and phosphorous contents suggest that this sample is an octahedrite or possibly a high phosphorous ataxite. Chemical analysis of the germanium, gallium and irridium contents will help define the classification more precisely.

3. Metallographic Examination

The large white areas visible (Fig. 1) even at low magnification are Fe-Ni phosphides surrounded by swathing kamacite.

Quantitative metallographic analysis indicated that about one-third of the total phosphorous content in the sample is contained in these very large regions which would form during cooling below 850°C.

A higher magnification photomicrograph of Yamato-75031 is shown in Fig. 2. The appearance of large phosphide areas and the swathing kamacite can be seen more clearly, and fine Widmanstätten kamacite plates may also be seen. These finer plates nucleated and formed at lower temperatures than the swathing kamacite which surrounds the coarse phosphides.

At higher magnification, as shown in Fig. 3, it may be seen that the coarse phosphide is surrounded by swathing kamacite which contains about 7.5% Ni according to the electron probe analysis. The kamacite is separated from the plessite by a very narrow nickel-rich rim of taenite. This taenite rim contains approximately 30% nickel. The plessite structure contains about 16% nickel kamacite and some residual untransformed taenite of about 30%Ni.

An example of Widmanstätten kamacite is shown in the photomicrograph in Fig. 4. The kamacite plates nucleate on phosphide particles, although the particle is not always evident within the plate if it is not in the polished surface. This kamacite is also rimmed with a nickel-rich taenite band. The transformation structure of the plessite can be seen more clearly in this micrograph.

The plessite structure is primarily composed of subgrains of 15–20%Ni kamacite but it is likely that there are small untransformed regions of fcc taenite containing some 25–30%Ni within the plessite. The appearance of this plessite structure indicates that there was very little reheating of this sample to modify the original transformation structure. The sample was analyzed for fcc and taenite content by measurement of the integrated X-ray intensities of fcc and bcc diffration peaks to determine the volume fraction of taenite. These measurements indicated a volume fraction of about 15% of fcc iron-nickel phase. The sample was rotated to ensure an accurate analysis as relative intensities of the peaks revealed that a strong crystallographic texture was present in keeping with the coarse grain size of the sample.

4. Discussion

The chemical composition of Yamato-75031 corresponds to either a very phosphorous-rich high-nickel ataxite or a plessitic octahedrite. However, the microstructure is clearly distinct from the characteristic criss-cross lamellar structure of octahedrites. Nor does the sample exhibit the usual appearance of an ataxite possibly because of the very high phosphorous content. However, it is quite similar in appearance to a Piñon meteorite found in New Mexico which has a composition of 16.2%Ni and 0.34%P (Buchwald, 1975). Piñon is classified as an anomalous nickel-rich ataxite resembling the ataxites of Group IVB but with ten times more Ga-Ge than usual.

In meteorites of this composition, (Fe, Ni)$_3$P, phosphide will begin to precipitate during cooling around 800–850°C. After cooling to about 600°C, swathing kamacite will nucleate at the taenite phosphide interface and grow to generally surround the phosphide particles which nucleated the kamacite as illustrated in Fig. 4. As cooling continues, the taenite at the rim of the kamacite becomes slightly enriched in nickel and depleted in phosphorous as has been discussed in detail by Goldstein and Ogilvie (1965), and Goldstein and Doan (1972). Precipitation of phosphide in the remaining taenite will continue as the solubility decreases during cooling from the original value of about 1% to less than 0.02% phosphorous below 500°C. Similarly, the solubility of phosphorous in kamacite decreases with temperature during cooling resulting in the precipitation of very

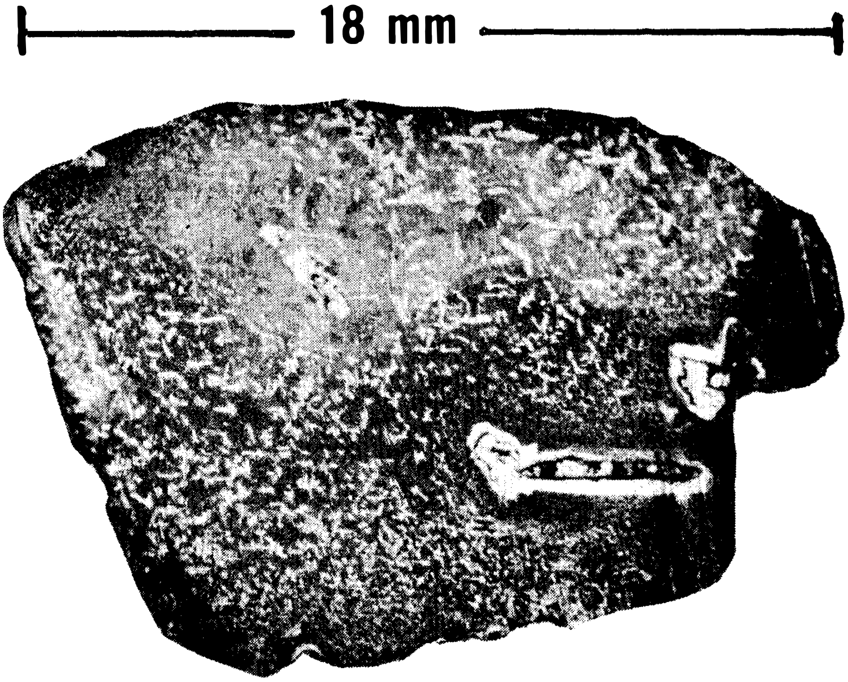

Fig. 1. Optical micrographs of full cross-section of Yamato-75031 showing kamacite and several large schreibersite particles $(Fe, Ni)_3P$.

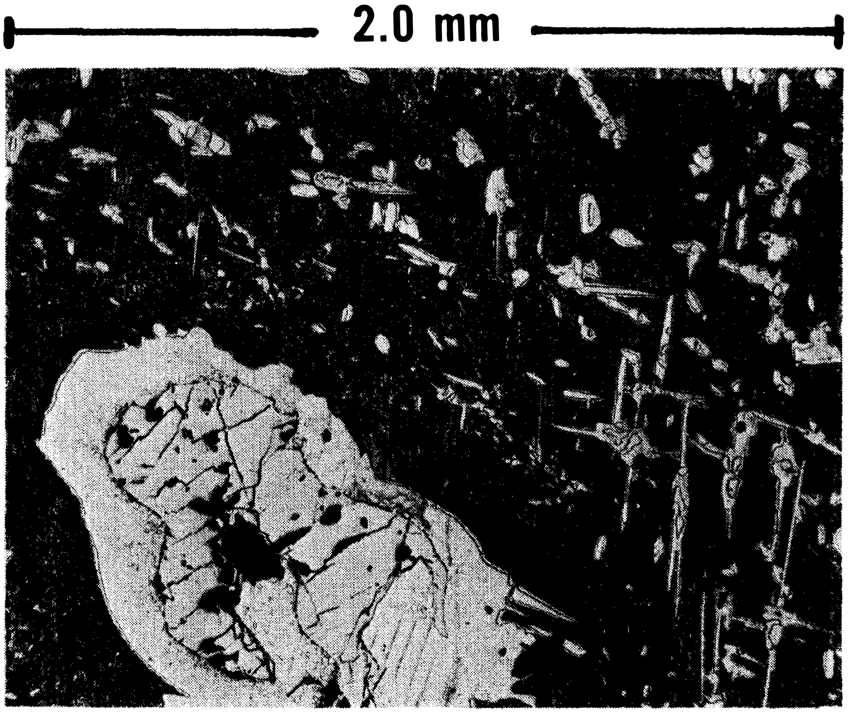

Fig. 2. Optical micrograph showing coarse schreibersite particle and swathing kamacite and fine Widmanstätten kamacite in plessite matrix (Yamato-75031).

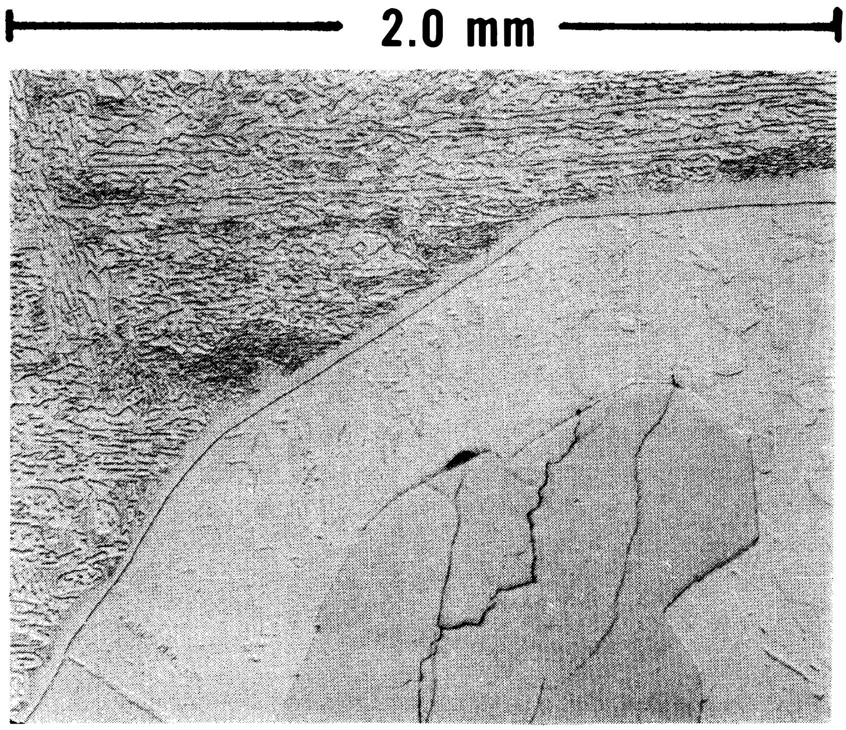

Fig. 3. Higher magnification shows that the coarse phosphide is surrounded by swathing kamacite (7.5%Ni, 0.2%P) containing very fine phosphide needles and a nickel-rich (~30%) rim of taenite (Yamato-75031).

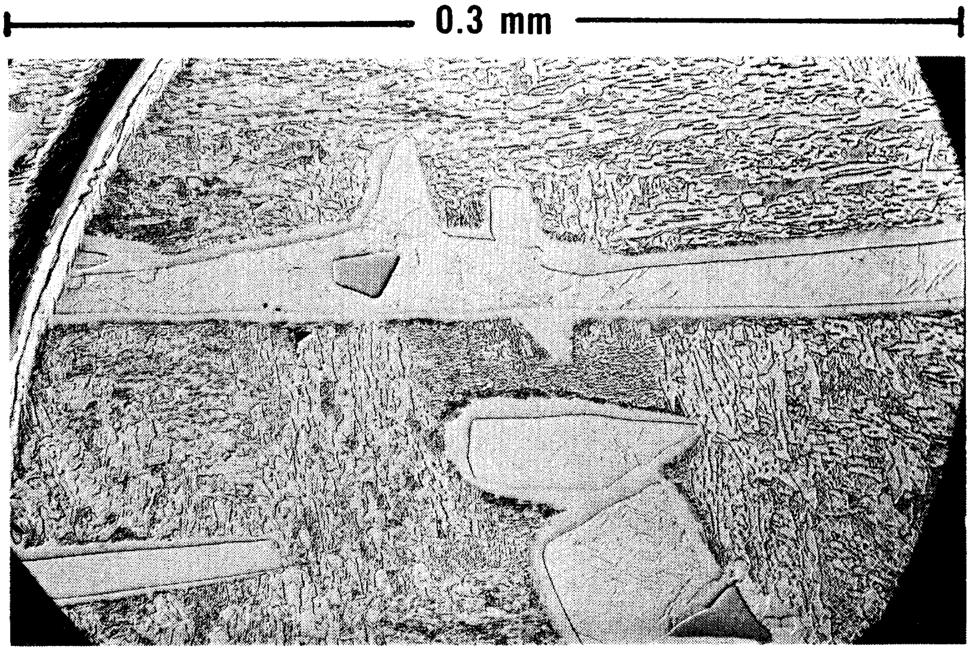

Fig. 4. Higher magnification shows that Widmanstätten kamacite particles nucleated on phosphides and are surrounded by a nickel-enriched rim. Fine phosphide particles may be seen in the kamacite. The transformation structure of the plessite is also evident (Yamato-75031).

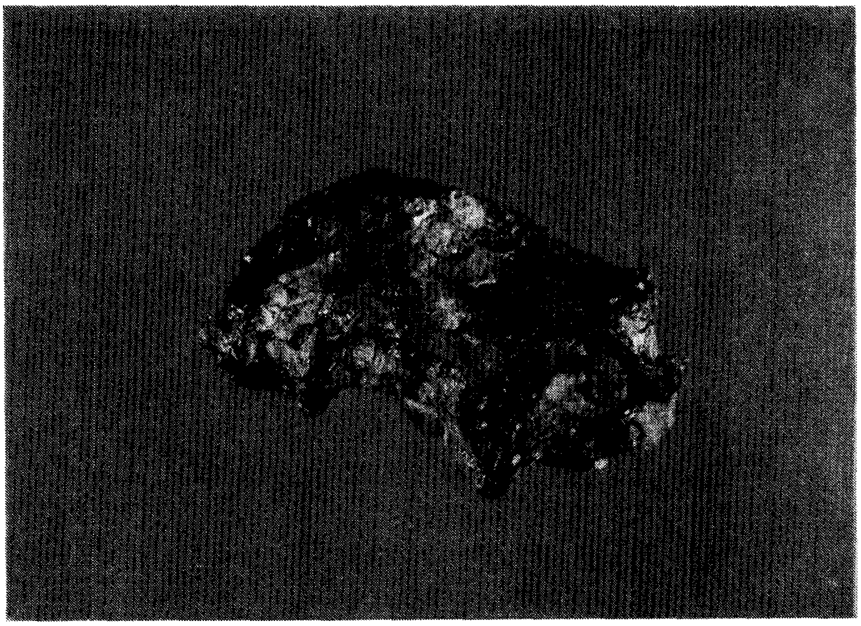

Fig. 5. Photograph of Yamato-74044 stony-iron meteorite prior to preparation of metallographic sections (approximately 1.5 times actual size).

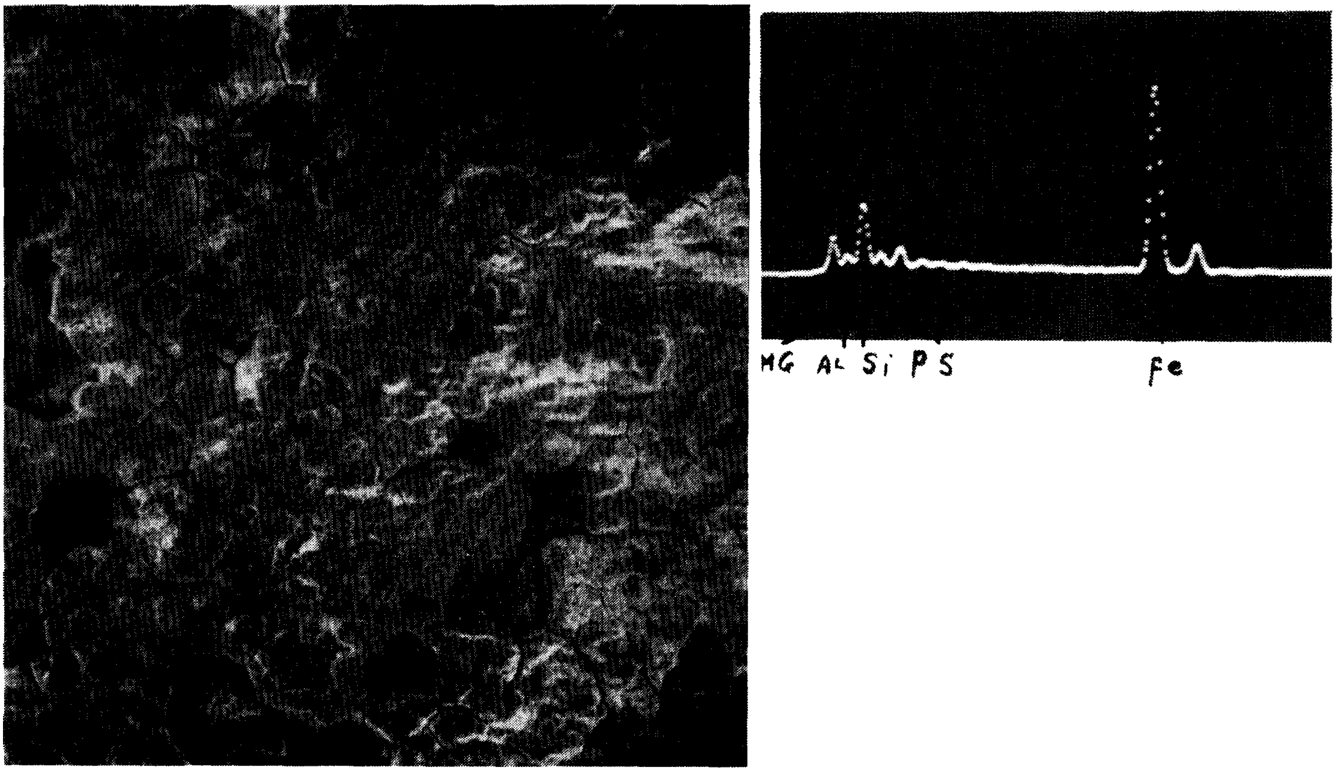

Fig. 6. Scanning electron micrograph of fusion crust of Yamato-74044 stony-iron meteorite. Insert X-ray spectra indicates approximate composition (1,000×).

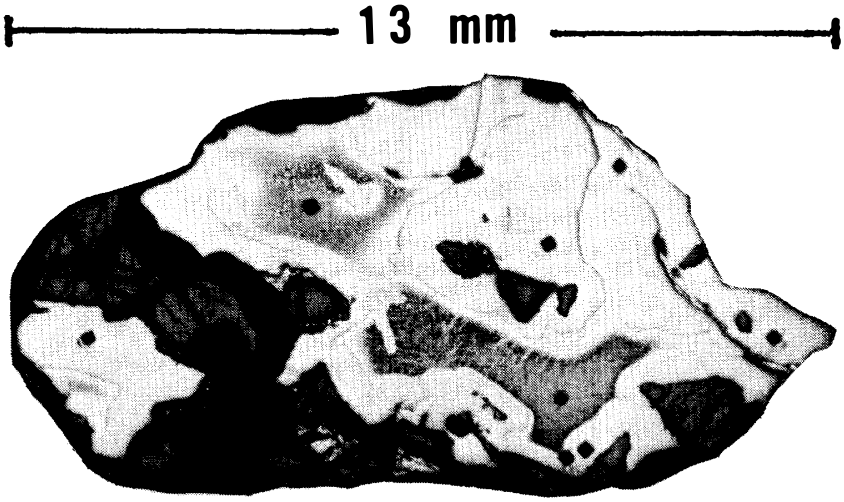

Fig. 7. Micrograph of cross-section of Yamato-74044 stony-iron meteorite showing ~11% nickel-iron and pools of olivine.

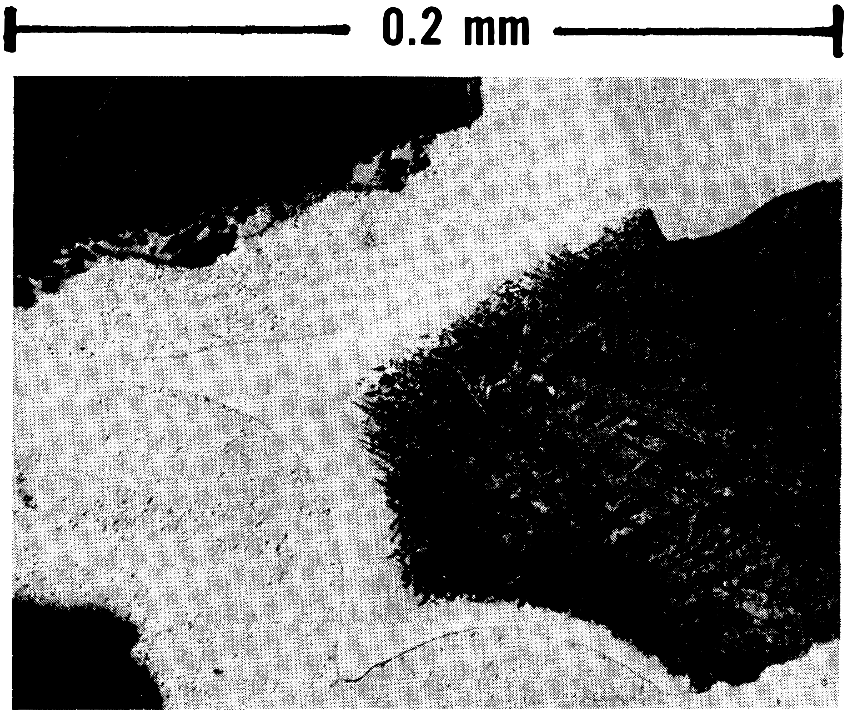

Fig. 8. Photomicrograph showing taenite-plessite band surrounded by kamacite (7%Ni). The nickel content of the rim is approximately 45% and declines to 20% in the dark-etching plessite (Yamato-74044).

fine phosphide particles in the kamacite as can be seen in the micrograph. This sequence of precipitation of phosphide over a wide temperature range gives rise to phosphide particle sizes varying from about 0.1 mm to less than 0.005 mm in width.

5. General Description of Yamato-74044

Yamato-74044 is an irregular peanut-shaped piece of stony-iron meteorite about 3 cm in length and about 4.7 cm in diameter, and is rather colorful with orange, blue and metallic flecks. A photograph of the examined piece is shown in Fig. 5. The weight of the sample as found was about 51.8 grams with an apparent density of 5.0833.

Scanning electron micrograph of the fusion crust from an exposed olivin area is shown in Fig. 6, along with the X-ray spectral lines from this region. It can be seen that the fusion crust contains silicon, iron, magnesium, aluminum, phosphorous, and sulphur in approximately the concentrations indicated.

The sample was sectioned and mounted for metallographic analysis. The full cross-section of the sample after polishing is shown in Fig. 7. Qualitative X-ray fluorescence analysis of the cross-section gave the following approximated chemical composition. (Because of the presence of both silicate and metallic phases corrections for fluorescence and adsorption could not be made so these compositions must be considered as approximate.)

Chemical composition.

	Si	Ni	Co	P	S	Al	Nb	Fe+O
Metal	3.2	10.6	0.75	0.1	0.1	0.5	0.02 (wt. %)	Remainder
		Mo, Cu, Cr, V, Ti, Mn<0.01						

Includes some small olivine regions; composition of metal is about 11.5% Ni.

The metallic structure may be seen somewhat more clearly at higher magnification in Fig. 8, showing kamacite adjacent to the pools of olivine, dark plessite within the taenite band and an etch-resistant rim of Ni-rich taenite. The chemical composition of the different regions was determined by qualitative electron probe analysis. The kamacite contains about 7%Ni, and the rim, at the outer surface, is enriched up to 45%Ni, and decreases to about 27%Ni at the edge of the plessite region.

The very fine structure within the plessite is due to a martensite-like transformation which occurs after cooling below about 200°C. The center of the taenite band at the middle of the plessite region contains about 20%Ni.

Microhardness measurements were taken on the different structural features shown in the micrograph. The hardness of the kamacite bands ranged from 159 to 166, whereas fine-grained kamacite regions showed hardnesses from 172 to 179. The plessite varied from 216 dph in the light plessite regions and increased to 253 in the dark plessite. The taenite rim is around 221, although this may have been influenced by the very closely adjacent harder plessite.

In terms of the customary meteorite classification system, the nickel and olivine content of this meteorite identifies it as a pallasite. WOOD (1967) has shown that the metal grains in stony-irons evolve *in situ* just as in octahedrites during cooling from metamorphic temperature. Thus, kamacite nucleated at the silicate, taenite interface and grew inward from this interface concentrating nickel into the remaining taenite. The kamacite composition is about 7%, and the band widths range up to about 0.2 mm. Iron sulfide veining is present within the silicate phase but to-date our metallographic examination has not concentrated on the silicate components.

6. Summary Discussion

The nickel content of the three iron or stony-iron meteorites, namely, Yamato-75105, Yamato-74044 and Yamato-75031, include three quite different ranges, *i.e.*, about 5.5% and 15.5% for the two iron samples and about 10.3% nickel for the stony-iron. The approximate cooling conditions for the three samples are shown in Fig. 9 superimposed on a pseudophase diagram for iron-nickel alloys prepared by GOLDSTEIN and DOAN (1970). In the case of Yamato-75105, transformation to form alpha plus phosphides occurs initially just above 900°C and transformation to kamacite is completed after cooling to about 600°C. In the case of the stony-iron sample, because of the higher nickel content, transformation began around 700°C, and during cooling the phosphorous content in the kamacite is reduced to below 0.25%. The nickel concentration in the gammaphase, formed as cooling continued below 400°C, will increase to 40–45%Ni which is in agreement with the measured values of the rims of the taenite bands.

Yamato-75031 which contains more than 15%Ni remained a face-centered taenite until it cooled below 650°C. After nucleation, kamacite continued to form down to about 500°C resulting in an enrichment in nickel content of the taenite to about 25%Ni, at which point the cooling rate must have increased and further transformation did not occur.

As discussed, the metallographic features are generally compatible with those expected to result from slow cooling for the different nickel-phosphorous contents of the three meteorites. However, reheating must have occurred and modified the original structure somewhat.

It is difficult to gauge the effects of reheating on such small meteorite samples. Pronounced microstructural changes in the heat affected rim on large meteorites only extends from 2 to 4 mm in thickness but the hardness is lowered due to annealing to a depth of as much as 10 mm. Thus the heat affected zone must extend completely across these samples. Considering both the appearance of the microstructure and the hardness, it is probable that the samples were heated to about 600°C for a few minutes.

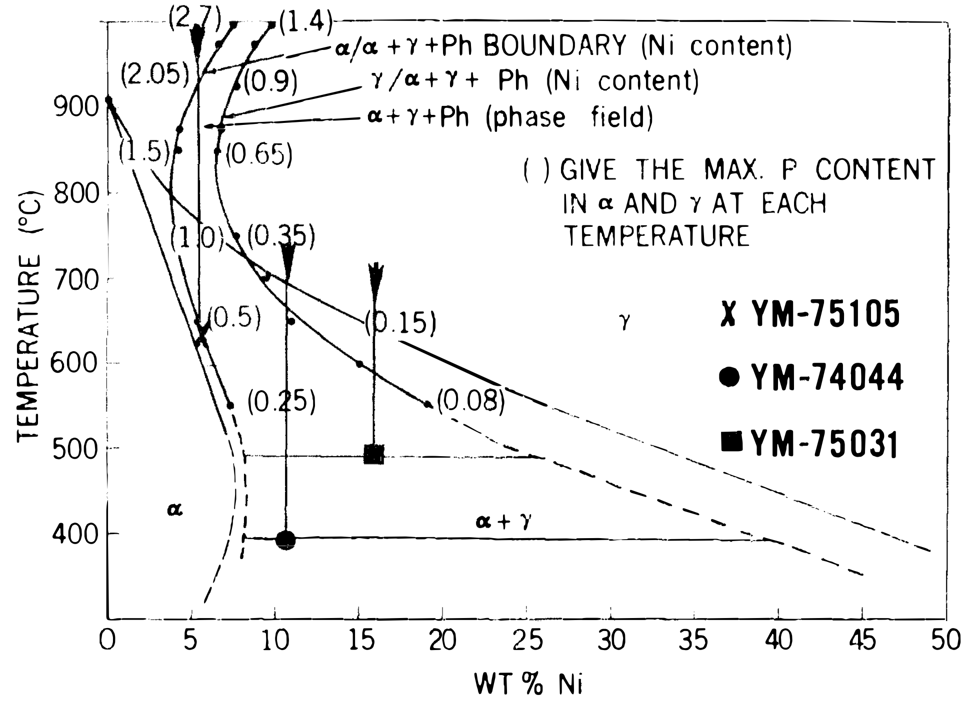

Fig. 9. Composition of Yamato iron meteorite superimposed on pseudo-binary phase diagram of **Doan** *and* **Goldstein** *(1970).*

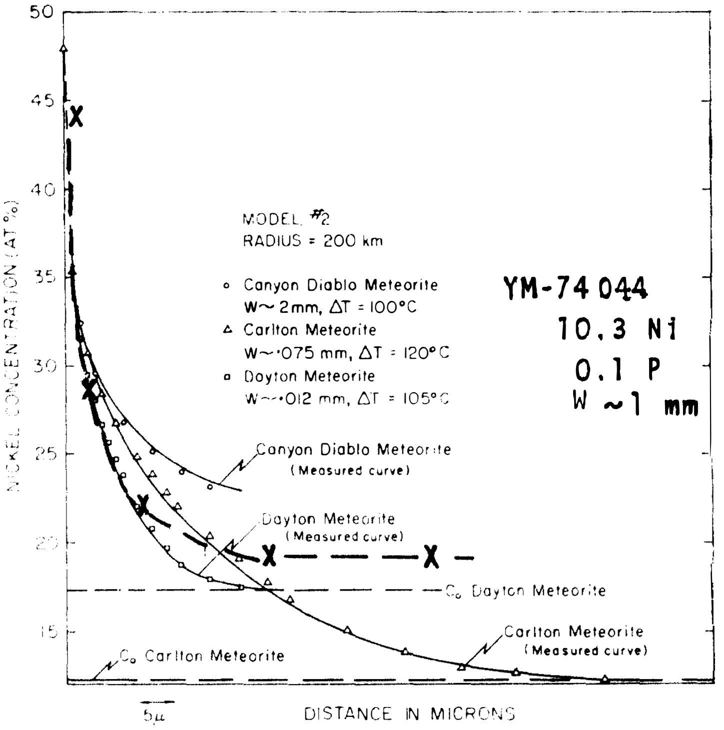

Fig. 10. Electron probe measurement of nickel concentration from taenite rim to center of plessite band superimposed on data published by **Goldstein** *and* **Ogilvie** *(1965).*

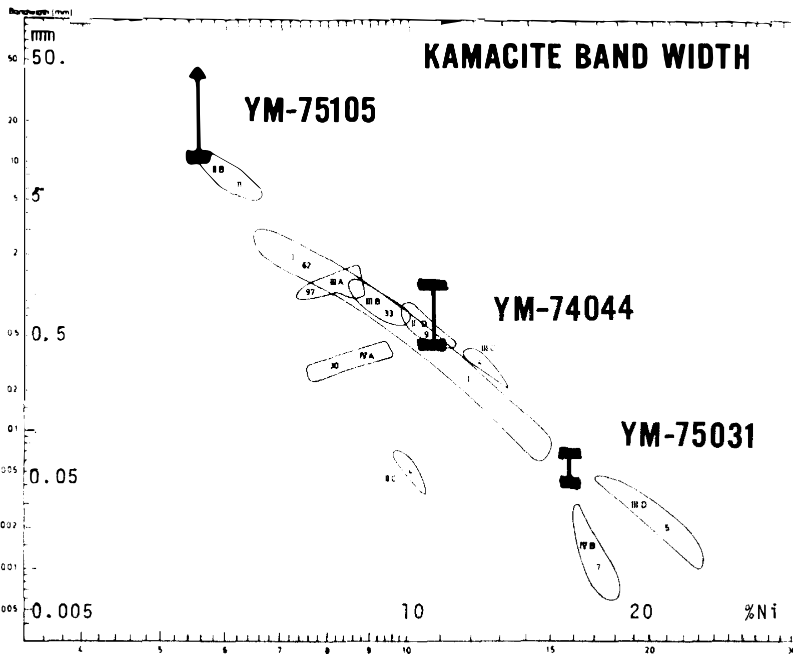

Fig. 11. Kamacite band width of Yamato iron meteorites superimposed on log-log plot of width vs. nickel content, published by BUCHWALD *(1975).*

The results of electron probe measurements across the taenite band in Fig. 8 is compared with the measurements and theory by GOLDSTEIN and OGILVIE (1965) in Fig. 10. These data refer to Yamato-74044 and are shown as X's on the figure. It is clear that the concentration profile falls in between Canyon Diablo and Dayton meteorites. The measured central plessite content rather close to 20%Ni and enriched rim of at least 45% compared favorably with the theoretical expectations based on the phase diagram for Fe-Ni alloys.

The kamacite band widths of the three Yamato metallic specimens vary considerably in keeping with their nickel content as expected. The measured values of the kamacite band widths are plotted in Fig. 11 in comparison with the collected data on band width as a function of nickel content reviewed in BUCHWALD's book on "Iron Meteorites". It may be seen that the three samples fall in the expected ranges based on their bulk nickel content. In the case of the Yamato-75105 sample, the kamacite band width can only be a lower limit because it corresponds to the full dimensions of the specimen.

The Yamato irons actually found are more than ten times smaller than any iron meteorites previously examined. Presumably small iron meteorites are not easily recognized on the earth's surface and are also destroyed by atmospheric corrosion more rapidly. Such samples are well preserved in the Antarctic and when exposed by ablation of the ice appear quite distinctive on the surface of the ice. Furthermore, artificial meteorite experiments suggest that very few meteorites of this size will not burn up during entry and reach the earth's surface. At any rate, discovery of only a few 20–60 gram irons is compatible with the size distribution data assembled by BUCHWALD (1975).

References

BUCHWALD, V. F. (1975): Handbook of Iron Meteorites, Their History, Distribution, Composition and Structure, Vols. 1–3. University of California Press.

GOLDSTEIN, J. I. and OGILVIE, R. E. (1965): The growth of the Widmanstätten pattern in metallic meteorites. Geochim. Cosmochim. Acta, **29**, 893–920.

GOLDSTEIN, J. I. and DOAN, A. S., Jr. (1972): The effect of phosphorus on the formation of the Widmanstätten pattern in iron meteorites. Geochim. Cosmochim. Acta, **66**, 51–69.

NAGATA, T., ed. (1975): Yamato Meteorites Collected in Antarctica in 1969. Mem. Natl Inst. Polar Res., Spec. Issue, **5**, 110 p.

NAGATA, T., FISHER, R. M. and SUGIURA, N. (1976): Metallographic and magnetic properties of a Yamato iron meteorite—Yamato-75105. Mem. Natl Inst. Polar Res., Ser. C, **10**, 1–11.

WOOD, J. A. (1967): Chondrites: Their metallic minerals, thermal histories, and parent planets. Icarus: Int. J. Solar System, **6**, 1–49.

YANAI, K. (1975): Chishitsu. Nihon Nankyoku Chiiki Kansokutai Dai-15-ji hokoku (Geology. Report of the 15th Japanese Antarctic Research Expedition), Tokyo, National Institute of Polar Research, 72–76.

(Received July 13, 1977)